

1 **The Capsid Protein of Semliki Forest Virus Antagonizes RNAi in**

2 **Mammalian Cells**

3

4 Qi Qian^{1,2}, Hui Zhou^{1,2}, Ting Shu^{2,3}, Jingfang Mu², Yuan Fang^{1,2}, Jiuyue Xu^{2,4}, Tao
5 Li^{2,4}, Jing Kong^{2,4}, Yang Qiu^{2,4*}, Xi Zhou^{1,2,4*}

6

7 1 State Key Laboratory of Virology, College of Life Sciences, Wuhan University,
8 Wuhan, Hubei, 430072 China

9 2 State Key Laboratory of Virology, Wuhan Institute of Virology, Center for
10 Biosafety Mega-Science, Chinese Academy of Sciences, Wuhan, Hubei, 430071
11 China

12 3 Center for Translational Medicine, Wuhan Jinyintan Hospital, Wuhan, Hubei,
13 430040, China

14 4 University of Chinese Academy of Sciences, Beijing, 100049 China

15 *To whom correspondence should be addressed. Tel/Fax: +86-27-87197080; E-mail:
16 yangqiu@wh.iov.cn (to Y.Q.); zhoxi@wh.iov.cn (to X.Z.)

17 Running Title: SFV capsid antagonizes RNAi in mammalian cells

18 **ABSTRACT**

19 RNA interference (RNAi) is a conserved antiviral immune defence in eukaryotes,
20 and numerous viruses have been found to encode viral suppressors of RNAi (VSRs)
21 to counteract antiviral RNAi. Alphaviruses are a large group of positive-stranded
22 RNA viruses that maintain their transmission and life cycles in both mosquitoes and
23 mammals. However, there is little knowledge about how alphaviruses antagonize
24 RNAi in both host organisms. In this study, we identified that Semliki Forest virus
25 (SFV) capsid protein can efficiently suppress RNAi in both insect and mammalian
26 cells by sequestering dsRNA and siRNA. More importantly, when the VSR activity
27 of SFV capsid was inactivated by reverse genetics, the resulting VSR-deficient SFV
28 mutant showed severe replication defects in mammalian cells, which could be rescued
29 by blocking the RNAi pathway. Besides, capsid protein of Sindbis virus (SINV) also
30 inhibited RNAi in cells. Together, our findings show that SFV uses capsid protein as
31 VSR to antagonize RNAi in infected mammalian cells, and this mechanism is
32 probably used by other alphaviruses, which shed new light on the knowledge of SFV
33 and alphavirus.

34 **Importance**

35 Alphaviruses are a genus of positive-stranded RNA viruses and include
36 numerous important human pathogens, such as Chikungunya virus, Ross River virus,
37 Western equine encephalitis virus, etc, which create the emerging and re-emerging
38 public health threat worldwide. RNA interference (RNAi) is one of the most
39 important antiviral mechanisms in plants and insects. Accumulating evidence has
40 provided strong support for the existence of antiviral RNAi in mammals. In response
41 to antiviral RNAi, viruses have evolved to encode viral suppressors of RNAi (VSRs)
42 to antagonize the RNAi pathway. It is unclear if alphaviruses encode VSRs that can
43 suppress antiviral RNAi during their infection in mammals. In this study, we first
44 uncovered that capsid protein encoded by Semliki Forest virus (SFV), a prototypic
45 alphavirus, had a potent VSR activity that can antagonize antiviral RNAi in the
46 context of SFV infection in mammalian cells, and this mechanism is probably used by
47 other alphaviruses.

48 **INTRODUCTION**

49 RNAi is a conserved post-transcriptional gene silencing mechanism that
50 originally evolves as an intrinsic antiviral immune mechanism in a broad range of
51 eukaryotic organisms (1-3). In the process of antiviral RNAi, the viral replicative
52 intermediate double-stranded RNAs (vRI-dsRNAs) synthesized during virus
53 replication are sensed and cleaved by host endoribonuclease Dicer into approximately
54 21- to 23-nucleotide (nt) virus-derived small interfering RNA (vsiRNA). These
55 vsiRNAs are then loaded into the Argonaute (AGO) protein of the RNA-induced
56 silencing complexes (RISCs) to mediate the cleavage of cognate viral genomic RNAs
57 (2, 4, 5). So far, RNAi has been widely recognized as the major antiviral response in
58 fungi, plants and insects (1, 2). For mammals, vRI-dsRNAs and other viral nucleic
59 acids usually induce innate antiviral immunity such as the type I interferon (IFN-I)
60 system (1). Recently, accumulating evidence have provided strong support for the
61 existence of antiviral RNAi in mammals (6-10).

62 In response to antiviral RNAi, viruses have evolved to encode VSRs to antagonize
63 the RNAi pathway through different mechanisms (11). Some VSRs bind to and
64 sequester long dsRNAs and/or siRNAs to shield them from Dicer cleavage or to
65 prevent their loading into AGO, while others inhibit certain important components of
66 the RNAi pathway such as Dicer or AGO (11). For instance, Flock house virus (FHV)
67 B2 acts as a VSR by preventing dsRNA from being cleaved by Dicer-2 as well as
68 sequestering the siRNAs produced by Dicer-2 (12-14), while Wuhan nodavirus B2
69 can directly bind and inhibit *Drosophila* Dicer-2 required for vsiRNA production (15,

70 16). Besides, cricket paralysis virus 1A directly inhibits the endonuclease activity of
71 AGO2 and simultaneously targets AGO2 for proteasomal degradation in *Drosophila*
72 (17).

73 In mammals, a number of viral proteins, such as Ebola virus VP35 (18), HIV-1
74 Tat (19), Hepatitis C virus core (20), Dengue virus NS4B (21), Yellow Fever virus
75 (YFV) capsid (22), and coronavirus 7a and nucleocapsid (23, 24), have been shown to
76 suppress ectopic dsRNA/shRNA-induced RNAi in *vitro*. On the other hand, a handful
77 of viral proteins encoded by mammalian viruses, including Enterovirus A71 (EV-A71)
78 3A, Influenza A virus NS1, and Nodamura virus (NoV) B2, have been found to act as
79 *bona fide* VSRs that antagonize antiviral RNAi in the course of viral infections (6, 8,
80 10).

81 Alphaviruses are a large group of positive-stranded RNA viruses that belong to
82 the genus *Alphavirus* in the family *Togaviridae* (25), and include numerous medically
83 important human pathogens such as Sindbis virus (SINV), Chikungunya virus
84 (CHIKV), Ross River virus, Eastern equine encephalitis virus, Western equine
85 encephalitis virus, Venezuelan equine encephalitis virus, etc. The infections by these
86 viruses are responsible for a broad spectrum of diseases, ranging from mild,
87 undifferentiated, febrile illness to debilitating polyarthralgia, encephalitis, and even
88 death in human and horses (26-29). To date, there is no approved antiviral therapy
89 specific for alphaviruses (30). Alphaviruses transmit between mosquito vectors and
90 vertebrate hosts (31, 32), and create emerging and re-emerging public health threat
91 worldwide (33). Although previous studies indicated the critical role of antiviral

92 RNAi in regulating the replication of alphaviruses such as CHIKV and SINV in
93 mosquitoes (31), it is unclear if alphavirus encodes a *bona fide* VSR that can suppress
94 antiviral RNAi during viral infection in mammals.

95 SFV is a member of the *Alphavirus* genus. Although SFV infection only causes a
96 mild febrile illness in human, it is highly pathogenic in rodents and serves a model
97 virus to investigate the mechanisms of viral replication, virus-host interaction, and
98 innate immunity (34-36). SFV contains a single positive-stranded RNA genome of
99 approximately 12 kb, which consists of two open reading frames (ORFs) that encode
100 four non-structural proteins (nsP1 to nsP4), three structural proteins (capsid, envelope
101 glycoproteins E1 and E2), and two small cleavage products (E3 and 6K) (36). Both
102 ORFs are translated as polyproteins, which undergo *cis* and *trans* cleavage to form the
103 mature viral proteins. SFV capsid protein is multifunctional and plays a critical role in
104 the encapsidation of genome and formation of viral nucleocapsid (37-39). In
105 this study, we first uncovered that SFV-encoded capsid protein had a potent *in vitro*
106 VSR activity that suppressed artificially induced RNAi in both insect and mammalian
107 cells. We further demonstrated that SFV capsid can act as *bona fide* VSR to
108 antagonize RNAi in the context of SFV infection in mammalian cells.

109 **RESULTS**

110 **SFV capsid protein is a potential VSR.**

111 To evaluate whether SFV encodes any protein that works as a potential VSR, we
112 examined all SFV-encoded proteins via a reversal-of-silencing assay in *Drosophila* S2
113 cells, which was previously used by us to screen VSRs of other viruses (15). In brief,
114 cultured S2 cells were co-transfected with the plasmid encoding EGFP and
115 EGFP-specific dsRNA, which is cleaved by fly Dicer-2 to produce siRNA and induce
116 RNAi, together with the plasmid encoding one of the SFV proteins (Fig. 1A). The
117 expression of the viral proteins was confirmed by Western blotting with anti-His
118 antibody (Fig. 1B). At 48 hour post transfection (h.p.t.), the mRNA levels of EGFP
119 were detected by Northern blotting with a DIG-labeled RNA probe targeting 520-700
120 nt of EGFP ORF. The EGFP-specific dsRNA can induce RNAi to destruct EGFP
121 transcript (Fig. 1A, lane 2). FHV B2 (FB2), a well-characterized VSR, was used as a
122 positive control, which expectedly restored EGFP mRNA levels (Fig. 1A, lane 3). Our
123 data show that the ectopic expression of SFV capsid protein effectively restored the
124 accumulation of EGFP mRNA (Fig. 1A, lane 8), indicating that SFV capsid protein is
125 a potential VSR.

126 To further confirm the VSR activity of SFV capsid, we examined whether capsid
127 could rescue the replication of a B2-deficient FHV RNA1 replicon (FR1 Δ B2) in S2
128 cells (13). This mutant replicon lost the ability to suppress RNAi, leading to a
129 defective self-replication of FHV RNA1 and subgenomic RNA3 in S2 cells (Fig. 1C,
130 compared lanes 1 and 2). Our data show that the replication defect could be partially

131 rescued by the ectopic expression of either FHV B2 or SFV capsid (Fig. 1C, lanes 3
132 and 4) or by the knockdown of fly AGO2 or Dicer-2 (Fig. 1C, lanes 5 and 6).

133 Because that RNAi pathway is conserved from insects to mammals, we sought to
134 determine whether SFV capsid can suppress RNAi in cultured human 293T cells via
135 the reversal-of-silencing assay, in which RNAi is induced by co-expressing EGFP
136 expression vector and EGFP-specific short hairpin RNA (shRNA). Our data show that
137 ectopic expression of SFV capsid effectively suppressed the shRNA-induced RNAi in
138 293T cells (Fig. 1D and E). Moreover, it was expectedly that ectopically expressing
139 NoV B2 (NB2), another well-established VSR, suppressed RNAi (Fig. 1D, lane 3).
140 Together, our data demonstrate that SFV capsid protein is a potential VSR that can
141 suppress RNAi in both insect and mammalian cells.

142 Capsid proteins from alphaviruses share high homology in amino acid sequences,
143 suggesting a conserved function (40). Thus, we examined the VSR activity of capsid
144 protein from SINV via the reversal-of-silencing assays in both *Drosophila* S2 and
145 human 293T cells, respectively. Our data show that SINV capsid inhibited RNAi in
146 both cells (Fig. 1F and G), suggesting that the *in vitro* VSR activity is a common
147 feature for alphaviral capsid proteins.

148

149 **SFV capsid suppressed Dicer-mediated siRNA production by sequestering**
150 **dsRNA.**

151 It is well established that dsRNA/shRNA-induced RNAi requires the
152 Dicer-mediated cleavage of dsRNA or shRNA into siRNA (1). To explore whether

153 SFV capsid can suppress this process, RNAs harvested from 293T cells co-expressing
154 EGFP expression vector and EGFP-shRNA together in the presence or absence of
155 SFV capsid were subjected to small RNA Northern blotting by using a DIG-labeled
156 RNA oligo probe targeting EGFP siRNA. As shown in Fig. 2A, the accumulation of
157 22-nt Dicer-cleaved siRNA product was reduced in cells overexpressing SFV capsid
158 compared to that in cells overexpressing empty vector, indicating that SFV capsid can
159 inhibit Dicer-mediated siRNA production. These results are consistent with the
160 observation that SFV capsid could effectively restore shRNA-mediated elimination of
161 EGFP transcript in 293T cells (Fig. 1D).

162 We sought to examine whether SFV capsid inhibits siRNA production by directly
163 binding to long dsRNA. To this end, we purified the recombinant MBP-fusion capsid
164 protein (MBP-capsid, Fig. 2B, lane 2) and conducted EMSA by incubating the *in vitro*
165 transcribed DIG-labeled 200-nt dsRNA together with MBP-capsid. As shown in Fig.
166 2C, capsid protein can bind to dsRNA directly and the shifting amount of labeled
167 dsRNAs was increased with the increasing amounts of MBP-capsid used in the
168 reaction. MBP-fusion FHV B2 (MBP-FB2) was used as positive control.

169 Subsequently, we sought to examine whether SFV capsid can protect dsRNA from
170 Dicer cleavage by using an *in vitro* RNase III assay (41). RNase III was widely used
171 as the Dicer substitute to examine the activities of VSRs as previously described (16).
172 Our data show that the presence of MBP-capsid efficiently protected dsRNA from
173 RNase III digestion in a dose-dependent manner (Fig. 2D, lanes 5-8), while dsRNA
174 was cleaved into siRNA in the presence of MBP alone (Fig. 2D, lane 2).

175 Altogether, our findings suggest that SFV capsid could suppress RNAi by
176 sequestering dsRNA from Dicer cleavage.

177

178 **SFV capsid suppressed siRNA-induced RNAi.**

179 In the RNAi pathway, when being processed from dsRNA, siRNAs are
180 incorporated into RISC to mediate the cleavage of cognate mRNAs (1). Since we
181 have found that SFV capsid can inhibit RNAi by sequestering dsRNA, it would be
182 intriguing to examine whether SFV capsid could also suppress siRNA-induced RNAi,
183 which is the step of post siRNA biogenesis. To this end, 293T cells were
184 co-transfected with a plasmid expressing EGFP and chemically synthesized
185 EGFP-specific siRNA (siEGFP), together with the expression vector for SFV capsid.
186 As shown in Fig. 3A, the chemically synthesized siRNA mediated the silencing of
187 EGFP mRNA, while SFV capsid efficiently restored the level of EGFP mRNA,
188 indicating that SFV capsid can suppress siRNA-induced RNAi in cells.

189 Because SFV capsid can suppress siRNA-induced RNAi, we speculate that
190 capsid protein may have siRNA-binding activity. To test this possibility, we
191 conducted EMSA by incubating purified MBP-capsid together with DIG-labeled
192 synthetic 22-nt siRNA. Our data show that SFV capsid protein can directly bind to
193 siRNA in a dose-dependent manner (Fig. 3B).

194 Taken together, our findings indicate that SFV capsid can suppress RNAi by
195 sequestering both dsRNA and siRNA.

196

197 **K124/K128 and K139/K142 of SFV capsid are critical for the VSR activity.**

198 After determining the *in vitro* VSR activity of SFV capsid, we sought to identify
199 the critical domain or amino acid (aa) required for its VSR activity. Previous studies
200 showed that SFV capsid consists of an N-terminal segment (aa 1-118) and a
201 C-terminal protease domain (aa 119-267) formed by two β -sheet domains (aa 119-181
202 and aa 182-267) (40). Accordingly, we constructed a set of capsid protein truncations,
203 as illustrated in Fig. 4A, and examined their activities to suppress RNAi via the
204 reversal-of-silencing assay in S2 cells. Our data show that the region of aa 119-181 is
205 critical for capsid's VSR activity (Fig. 4A). The expression of capsid protein
206 truncations was confirmed by Western blotting with anti-His antibody (Fig. 4B).

207 To identify the critical residue(s) within the aa 119-181 region required for the
208 VSR activity, we performed multiple sequences alignments of capsids encoded by
209 RRV, SFV, SINV and CHIKV. The conserved positively charged residues, lysine (K)
210 and aspartic acid (D), were subjected to single-point or double-point mutations to
211 Alanine (A), and the resulting mutant capsid proteins were then examined via the
212 reversal-of-silencing assay in S2 cells. Although none of the single-point mutations
213 disrupted the VSR activity (Fig. 4C and D), the K124A/K128A or K139A/K142A
214 mutation (capsid_{K124A/K128A} or capsid_{K139A/K142A}) significantly suppressed the activity
215 of SFV capsid to suppress RNAi (Fig. 4E, lanes 7 and 8; Fig. 4F and G) in S2 cells. In
216 addition, the truncation mutations (M2 and M3) and capsid_{K124A/K128A} or
217 capsid_{K139A/K142A} also lost the VSR activity in 293T cells (Fig. 4H and I). We also
218 found that the K124A/K128A or K139A/K142A mutation significantly

219 suppressed the activity of SFV capsid to suppress siRNA-induced RNAi in 293T cells
220 (Fig. 4J and K).

221 Moreover, we found that either K124A/K128A or K139A/K142A mutation
222 abolished the dsRNA- and siRNA-binding activities of SFV capsid (Fig. 5A and B).
223 Interestingly, although capsid_{K124A/K128A} and capsid_{K139A/K142A} failed to bind to dsRNA
224 or siRNA, their activities to bind to ssRNA were still intact (Fig. 5C).

225 Together, these data show that the K124A/K128A and K139A/K142A residues
226 are critical for the dsRNA/siRNA-binding and VSR activities of SFV capsid.

227

228 **Construction and recovery of VSR-deficient SFV.**

229 To find out whether SFV capsid protein indeed suppresses antiviral RNAi during
230 virus infection, we introduced the K124A/K128A and K139A/K142A mutation into
231 the capsid coding region of the infectious clone of SFV (Fig. 6A). The wild-type
232 (SFV_{WT}) and K124A/K128A mutant (SFV_{K124A/K128A}) viruses were successfully
233 recovered and the plaque morphology of these two viruses was similar (Fig. 6B),
234 whereas K139A/K142A mutant virus displayed lethal phenotype.

235 Because alphaviral capsid protein is critical for the formation of nucleocapsid
236 and virion maturation, we sought to exclude the possibility that the K124A/K128A
237 mutation may affect other important functions of SFV capsid, such as the process of
238 virion assembly and the virus entry into cells. Our previous data showed that SFV
239 capsid_{K124A/K128A} still kept the ssRNA-binding activity (Fig. 5C), implying that the
240 interaction between SFV capsid_{K124A/K128A} and viral genomic RNAs, which is

241 important for nucleocapsid assembly, is not affected. Moreover, we purified the
242 virions of SFV_{WT} and SFV_{K124A/K128A}, and then examined the morphology of both WT
243 and mutant virions via transmission electron microscopy (TEM). Our results showed
244 that the K124A/K128A mutation did not affect the morphology and diameter of viral
245 particles (Fig. 6C).

246 Subsequently, we sought to determine whether the K124A/K128A mutation
247 affected the entry efficiency of SFV into cells. To this end, 293T cells were infected
248 with SFV_{WT} or SFV_{K124A/K128A} at a multiplicity of infection (MOI) of 5, and at 15, 30
249 and 45 min post infection, the viruses remaining in the supernatant and the viral
250 RNAs within cells were examined by plaque assays and qRT-PCR, respectively. Our
251 data show that the levels of the remaining virions in the supernatant and the viral
252 RNAs within cells of SFV_{K124A/K128A} were comparable to those of SFV_{WT} at each time
253 point (Fig. 6D), indicating that the K124A/K128A mutation did not affect the entry of
254 SFV into cells.

255 After determining that the K124A/K128A mutation did not affect the virion
256 assembly and viral entry of SFV, we determined the one-step growth curve of WT and
257 mutant viruses in human 293T cells, showing that SFV_{K124A/K128A} exhibited weaker
258 growth patterns than did SFV_{WT} in 293T cells (Fig. 6E). This result indicates that the
259 inactivation of VSR function led to the restricted replication of SFV.

260

261 **The replication defect of VSR-deficient SFV can be rescued by the deficiency of**
262 **RNAi in 293T cells.**

263 To further explore the VSR function of SFV capsid during viral infection, 293T
264 cells were infected with WT or VSR-deficient SFV, and viral RNA accumulation
265 were determined at 6, 12, 24 hour post infection (h.p.i.), respectively. As expected, the
266 viral RNA accumulation of SFV_{K124A/K128A} was lower than that of SFV_{WT} in 293T
267 cells (Fig. 7A). The genetic ablation of the RNAi pathway by Dicer knockout in 293T
268 cells (NoDice) rescued the replication of SFV_{K124A/K128A} (Fig. 7A). Interestingly, the
269 RNA accumulation of SFV_{K124A/K128A} was significantly reduced in 293T cells treated
270 with enoxacin compared to that in the controlled 293T cells (Fig. 7B). Of note,
271 enoxacin is a well-known RNAi enhancer and functions at steps post siRNA
272 production by Dicer in the RNAi pathway (9, 42). Expectedly, ectopic expression of
273 human Dicer (hDicer) in 293T-NoDice cells resulted in the reduced RNA
274 accumulation of SFV_{K124A/K128A} (Fig. 7B and C).

275 Moreover, the viral RNA replication of SFV_{K124A/K128A} in 293T cells was
276 increased by the ectopic expression of SFV capsid or NoV B2, but not the
277 VSR-deficient mutant of capsid (capsid_{K124A/K128A}) or NoV B2 (B2_{R59Q}, named as
278 mB2) (Fig. 7A and D). And the rescuing effect of ectopically expressed capsid on the
279 replication of VSR-deficient SFV was confirmed by using Northern blotting with a
280 DIG-labeled RNA probe that recognized both genomic and subgenomic RNAs of
281 SFV (Fig. 7E).

282 Furthermore, we found that ectopic expression of NoV B2 or SFV capsid could
283 not rescue the RNA accumulation of SFV_{K124A/K128A} in 293T-NoDice cells (Fig. 7F
284 and G). These results indicate that the rescuing effect of ectopically expressed foreign

285 VSRs on the replication of SFV_{K124A/K128A} is indeed RNAi-dependent.

286 To exclude the potential impact of IFN-I response, we treated 293T or
287 293T-NoDice cells infected by SFV_{K124A/K128A} with Ruxolitinib, a JAK1 and JAK3
288 inhibitor, to block IFN-I. We found that ectopic expression of foreign VSRs or
289 deficiency of Dicer could still enhance the RNA accumulation of SFV_{K124A/K128A} in
290 Ruxolitinib-treated cells (Fig. 7H and I), confirming that the rescuing effect is
291 irrespective of IFN-I.

292 In addition, we examined the production of vsiRNAs in SFV_{K124A/K128A}-infected
293 *Aedes* mosquito Aag2 cells. The Deficiency of VSR also resulted in substantial
294 attenuation of viral RNA accumulation of SFV_{K124A/K128A} in Aag2 cells (Fig. 7J),
295 consistent with the findings in 293T cells. SFV vsiRNAs in Aag2 cells were detected
296 via Northern blotting with RNA probe complementary to 3'-end 1-50 nt of the
297 negative-stranded antigenomic RNA. Our findings showed that the production of SFV
298 vsiRNAs was dramatically enhanced in Aag2 cells infected with SFV_{K124A/K128A} but
299 not SFV_{WT} (Fig. 7K).

300

301 **DISCUSSION**

302 Alphaviruses infect and replicate in both invertebrate vectors and mammalian
303 hosts. Efficient transmission of these viruses depends on their activities to counteract
304 the antiviral immune response in both mosquito vectors and human hosts (31). RNAi
305 is an antiviral immune response conserved in both invertebrates and mammals, while
306 many viruses encode VSRs as the countermeasure (2, 5). However, it was still unclear

307 if alphavirus encodes a VSR to antagonize antiviral RNAi in the context of viral
308 infection in mammalian cells. To date, the identification of a *bona fide* VSR encoded
309 by a mammalian virus requires to answer the following questions: 1) if disabling VSR
310 by reverse genetic can cause viral replication defect during authentic viral infection; 2)
311 if the genetic ablation of the RNAi pathway can rescue the replication defect of the
312 VSR-disabled mutant virus.

313 In the present study, we screened the viral proteins of SFV, a prototypic
314 alphavirus, for VSR activity in insect and mammalian cells. We found that SFV
315 capsid protein possesses VSR activity. The *in vitro* EMSA analysis shows that SFV
316 capsid has both dsRNA- and siRNA-binding activities that are indispensable for its
317 VSR function. More importantly, the VSR deficiency of SFV capsid resulted in
318 substantial restriction of viral replication in mammalian cells. And this
319 defective-replication of VSR-deficient mutant SFV can be rescued by the deficiency
320 of RNAi by either ectopically expressing foreign VSRs or blocking the RNAi
321 pathway, which is irrespective of the IFN-I system. In addition, when the
322 capsid-mediated RNAi suppression was genetically disabled in SFV, the production
323 of vsiRNAs was enhanced in infected mosquito cells. Thus, we propose a hypothesis
324 that SFV capsid may protect viral RNA from antiviral RNAi at two stages: (i)
325 blocking vRI-dsRNA from Dicer cleavage through dsRNA-binding activity; and (ii)
326 binding to vsiRNA to suppress in the incorporation of vsiRNA to RISC (Fig. 8).

327 In addition to SFV capsid, a remaining question is that if alphaviruses encode
328 another VSR(s). Previous study has identified CHIKV nsP2 and nsP3 suppressed

329 shRNA-induced RNAi in insect and mammalian cells (43). However, the potential
330 VSR activity of nsP2 and nsP3 was not tested in the context of an authentic viral
331 infection. Over-expression of any protein with an effective dsRNA- or siRNA-binding
332 activity may suppress RNAi in some cases, which does not mean that it acts as a VSR
333 during viral infection. In addition, viruses may encode more than one VSR, as seems
334 to be the case for some plant viruses, such as citrus tristeza virus (p20, p23 and coat
335 protein) (44) and potyviruses (P1 and HcPro) (45).

336 Alphaviral RNA packaging requires active viral RNA synthesis, implying that the
337 replication and encapsidation are tightly connected (46). This may explain why only
338 the genomic RNA can be specifically packaged into the virion, and suggests that
339 alphaviral structural proteins could directly involve in viral RNA replication. Indeed,
340 SFV capsid is a versatile structure protein that can bind to the large ribosomal subunit
341 in the cytoplasm and associate with the viral RNAs to form the viral nucleocapsid (38,
342 39). In this current study, we provided evidence that SFV capsid is a potent VSR,
343 which plays an important role in the viral RNA replication in insect and mammalian
344 cells. Our findings are consistent with the previous findings that VSR activities were
345 observed in viral structural coat proteins encoded by numerous viruses, including
346 Turnip crinkle virus coat protein, YFV capsid protein and coronavirus nucleocapsid
347 protein, and their VSR activities have been found to be associated with their
348 dsRNA-binding capacities (22, 24, 47).

349 SFV capsid is made up of two domains, the RNA binding N-terminal segment
350 (aa 1-118) and the C-terminal globular protease domain (aa 119-267), which is critical

351 for the dimerization of capsid (40). Indeed, our mutational analyses showed that
352 mutations of K124A/K128A or K139A/K142A abolished the dsRNA-/siRNA-binding
353 of SFV capsid but not ssRNA-binding activities. This data indicates that these
354 residues are not directly involved in the association of SFV capsid with viral genomic
355 RNAs, but possibly in the process of protein dimerization. Our results are consistent
356 with the previous findings that dimerization is required for RNAi suppression
357 activities of many VSRs, such as NoV B2 and EV-A71 3A (8, 48). The future work
358 will demonstrate the relationship between the VSR activity and the dimerization of
359 SFV capsid.

360 In summary, our study demonstrates that SFV capsid functions as a VSR in
361 facilitating viral replication by blocking either dsRNA from Dicer cleavage or
362 vsRNA loading into RISC in mammalian cells. Moreover, it shows for the first time
363 that an alphavirus can antagonize antiviral RNAi in the context of viral infection,
364 extending our knowledge about the interaction between alphavirus and antiviral RNAi
365 immunity.

366

367

368 **MATERIALS AND METHODS**

369 **Plasmids and RNAs**

370 For the expression of SFV proteins, their ORFs were cloned into insect expression
371 vector pAc5.1/V5-HisB, respectively. To express proteins in 293T cells, the ORF of
372 SFV capsid was constructed into the pRK-Flag. The full-length cDNA of the FHV

373 RNA1 and FHV RNA1 Δ B2 were described previously (24). For the purification of
374 the MBP fusion capsid protein, its ORF was inserted into the pMAL-c2X vector. The
375 enhanced green fluorescent protein (EGFP)-siRNA (siEGFP) was chemically
376 synthesized by Rui Bo, Guangzhou, China. The full-length SFV cDNA clone (strain
377 SFV4) was constructed in pCMV-Myc vector driven by CMV promoter (kindly
378 provided by Dr. Tero Ahola, University of Helsinki).

379

380 **Cell culture**

381 HEK293T cells were maintained in Dulbecco modified Eagle medium (DMEM)
382 supplemented with 10% fetal bovine serum (FBS) (GIBCO), 100 U/ml penicillin and
383 100 μ g/ml streptomycin at 37°C in an incubator with 5% CO₂. The 293T-NoDice cell
384 line was kindly provided by Dr. Bryan R. Cullen (Durham, NC, USA). *Drosophila* S2
385 or Aag2 cells were cultured in Schneider insect medium with 10% FBS at 27°C.
386 Before transfection with FuGene HD reagent (Roche, Basel, Switzerland), the
387 medium was changed to DMEM or Schneider insect medium containing 2% FBS
388 without any antibiotic. Cells were harvested at 48 h.p.t..

389

390 **Construction and recovery of SFV mutant virus**

391 To construct the SFV mutant clone, we obtained 6636-8748 nt of the full-length
392 cDNA clone via PCR, and cloned it into the pMd-18T vector. Then, the
393 K124A/K128A and K139A/K142A mutations were introduced into this plasmid via
394 over-lap PCR. The resulting mutant fragments were inserted into the full-length

395 cDNA clone by double enzyme digestion (Sbf I and Xba I). These infectious cDNA
396 clones were then transfected into the 293T cells using the FuGene HD reagent (Roche,
397 Basel, Switzerland), and the rescued viruses were harvested 48 h.p.t.. The virus titers
398 were measured by plaque assays.

399

400 **Western blotting**

401 Cells were harvested in lysis buffer [50 mM Tris-HCl (pH 7.4), 150 mM NaCl, 1%
402 NP-40, 0.25% deoxycholate and a protease inhibitor cocktail (Rhoche)]. Then the
403 lysates were subjected to 12% SDS-PAGE and Western blotting according to our
404 standard procedures (49). The antibodies used in this study are as follow: anti-Tubulin
405 (Protein Tech Group, 1:3000), anti-His (Protein Tech Group, 1:10000), anti-Flag
406 (Protein Tech Group, 1:5000), anti-Dicer (Protein Tech Group, 1:2000).

407

408 **Northern blotting and qRT-PCR**

409 Total RNAs were extracted using Trizol reagent (Thermo) according to the
410 manufacturer's instructions. For the detection of EGFP mRNA, 5 µg of total RNAs
411 were subjected to denatured 1.5% agarose gels with 2.2 M formaldehyde. The
412 separated RNAs were transferred onto the Hybond-A nylon membrane (GE
413 Healthcare) and fixed by 120°C for 15 min. Then the membranes were hybridized
414 with digoxigenin (DIG)-labeled probes in Hybridization Ovens at 65°C overnight.
415 The membranes were then incubated with anti-DIG antibody conjugated with alkaline
416 phosphatase, and exposed to the luminescent image analyzer LAS4000 (Fuji Film).

417 The probes for detection of EGFP, Rp49 and GAPDH mRNA were complementary to
418 520-700 nt, 273-490 nt and 760-1060 nt of their ORF regions, respectively. The probe
419 for detection FHV RNA1 and subgenomic RNA3 were complementary to 2738-3058
420 nt of B2 coding region. The probe for detection SFV genome and subgenomic RNA
421 were complementary to 723-1314 nt of E2 protein coding region. These probes were
422 labeled with DIG-UTP (Roche) by *in vitro* transcription. For detection of small RNAs,
423 20 µg of total RNAs were subjected to 7 M urea-15% PAGE and transferred to
424 Hybond-A nylon membrane (GE Healthcare). The membrane was chemically
425 cross-linked in 1-ethyl-3-(3-dimethylaminopropyl) carbodiimide (EDC) at 60°C. For
426 detection of vsiRNA, Aag2 cells were infected with SFV_{WT} or SFV_{K124A/K128A} at an
427 MOI of 10 for 24 h.p.t., then the total RNAs were subjected to 7 M urea-15% PAGE
428 for Northern blotting analysis. The probes targeting EGFP siRNA, U6 and vsiRNA
429 were synthesized by Takara, and their sequences were listed in Table 1. qRT-PCR
430 using SYBR mix (Takara) was carried out to detect the expression of EGFP mRNA,
431 β-actin mRNA and SFV NS1 mRNA. The primes and oligonucleotides used in this
432 study are shown in Table 1.

433

434 **Expression and purification of capsid protein**

435 The coding regions of SFV capsid protein and FHV B2 were cloned into pMAL-c2X.
436 Then *Escherichia coli* BL21 (Invitrogen) transformed with the expression plasmids
437 were grown to the log phase at 37°C and induced with 0.8 mM IPTG
438 (isopropyl-β-D-thiogalactopyranoside) at 22°C for 6 h. Thus, cells were harvested by

439 centrifugation and resuspended in lysis buffer [1 M Tris-HCl (pH 7.5), 0.2 M NaCl,
440 0.5 M EDTA (pH 8.0), 10 mM β -mercaptoethanol, 5% absolute ethylalcohol, 10%
441 glycerinum] and followed by sonication and centrifugation to remove the debris.
442 Finally, the proteins in the supernatant were purified using Amylose Resin (New
443 England BioLabs) according to the manufacturer's instructions.

444

445 **Electrophoretic mobility shift assay (EMSA) and RNase III cleavage assays**

446 MBP-fusion capsid was reacted with DIG-labeled RNAs (0.5 μ M 200-nt dsRNA, 0.5
447 μ M 200-nt ssRNA or 1 μ M 22-nt siRNA.) in a reaction buffer containing 40 mM
448 $MgCl_2$, 50 mM NaCl, 25 mM HEPES (pH 7.5), 3 mM dithiothreitol (DTT) and 1 U of
449 RNase inhibitor; the total volume is 10 μ L. After incubation for 30 min at 25°C, the
450 reaction mixtures were subjected to 1.5% native-TBE agarose gel and then transferred
451 to Hybond-A nylon membrane (GE Healthcare). The membranes were washed with
452 maleic acid buffer for 10 min, and then incubated with anti-DIG antibody conjugated
453 with alkaline phosphatase (Roche) for 30 min.

454 For the RNase III cleavage assay, 1 μ M 200-nt dsRNA was incubated with 1 U
455 RNase III (Invitrogen) and MBP-fusion proteins in reaction buffer according to the
456 manufacturer's instructions at 37°C for 30 min. The mature siRNAs processed by
457 RNase III were extracted from the reaction complex by using Trizol reagent (Thermo)
458 and subjected to 7 M urea-15% PAGE and then transferred to Hybond-A nylon
459 membrane (GE Healthcare).

460

461 **Virus infection and plaque assays**

462 At the day of infection, the medium was changed with 2% FBS DMEM and then
463 viruses were added in to 293T or Aag2 cells at an MOI of 1. Total RNAs were
464 extracted at 6, 12 and 24 h.p.i., and subjected to Northern blotting and qRT-PCR
465 analysis, respectively. For the rescue experiments, 293T cells were first transfected
466 with the plasmid encoding the indicated proteins, respectively for 24 h.p.t. and treated
467 with Ruxolitinib (10 μ M, Selleck) or Enoxacin (100 μ M, Selleck) for 1 h, and then
468 infected with viruses. To examine the entry efficiency of SFV into cells, 293T cells
469 were infected with WT or mutant SFV at an MOI of 5, and at 15, 30 and 45 min post
470 infection, the viruses remaining in the supernatant and the viral RNAs invaded into
471 cells were examined by plaque assays and qRT-PCR, respectively.

472 For plaque assays, Vero cells in 12-well plates were infected with 10-fold serial
473 dilution of viruses. Cells were cultured at 37°C for 2 h to allow the adsorption of all
474 the viruses. Then the supernatant was replaced with 1 \times MEM containing 2% FBS and
475 1% Penicillin-Streptomycin with isopyknic 1% low-melting-point agarose
476 (Sigma-Aldrich). After incubation at 37°C for 72 h, cells were fixed with 10%
477 formaldehyde and stained with 0.5% crystal violet at 4°C for 2 h.

478

479 **Sucrose density gradient ultracentrifugation and transmission electron**
480 **microscopy**

481 The cellular supernatant was filtrated by using the 0.45 μ m filtering membrane and
482 subjected to ultracentrifugation of 150000 g for 3 h at 4°C in a rotor SW28. After

483 centrifugation, the precipitate was resuspended in NTE buffer [10 mM Tris-HCl (pH
484 7.5), 120 mM NaCl, 1 mM EDTA] and then put into 10%-60% continuous sucrose
485 gradient for ultracentrifugation of 150000 g for 3 h at 4°C in a rotor SW41. The
486 sucrose solution of 30% and 40% containing virions were collected and further
487 subject to ultracentrifugation of 150000 g for 2 h at 4°C in a rotor SW41. In the end,
488 the precipitate was resuspended in 50 μ L NTE buffer.

489 For the transmission electron microscopy (TEM), virions were adsorbed to
490 glow-discharged electron microscope grids and negatively stained with the purified
491 terephthalic acid according to our standard procedures (50). Samples were imaged on
492 100KV, HITACHI H-7000FA TEM.

493

494 **ACKNOWLEDGMENTS**

495 We are grateful to Drs. Tero Ahola (Helsinki, Finland) and Bryan R. Cullen
496 (Durham, NC, USA) for reagents, and Pei Zhang and An-na Du from the Core
497 Facility and Technical Support, Wuhan Institute of Virology, for their help with
498 producing TEM micrographs.

499 This work was supported by the Strategic Priority Research Program of Chinese
500 Academy of Sciences (XDB29010300 to X.Z.), the National Natural Science
501 Foundation of China (81873964 to Y.Q., 31800140 to J.M., 31670161 to X.Z.), the
502 Science and Technology Bureau of Wuhan (2018060401011309 to X.Z.), the
503 Advanced Customer Cultivation Project of Wuhan National Biosafety Laboratory
504 (2018ACCP-MS11 to Y.Q.), and the Yunde Hou Academician Fund from National

505 Institute For Viral Disease Control and Prevention (2019HYDQNJJ10 to J.M.). X.Z.
506 is supported by the Newton Advanced Fellowship from the Academy of Medical
507 Sciences, UK (NAF005\1002).

508

509

510 REFERENCES

- 511 1. **Ding SW.** 2010. RNA-based antiviral immunity. *Nat Rev Immunol* **10**:632-644.
- 512 2. **Guo Z, Li Y, Ding SW.** 2019. Small RNA-based antimicrobial immunity. *Nat Rev Immunol*
513 **19**:31-44.
- 514 3. **Blair CD.** 2011. Mosquito RNAi is the major innate immune pathway controlling arbovirus
515 infection and transmission. *Future Microbiol* **6**:265-277.
- 516 4. **Aliyari R, Wu Q, Li HW, Wang XH, Li F, Green LD, Han CS, Li WX, Ding SW.** 2008. Mechanism
517 of induction and suppression of antiviral immunity directed by virus-derived small RNAs in
518 *Drosophila*. *Cell Host Microbe* **4**:387-397.
- 519 5. **Maillard PV, van der Veen AG, Poirier EZ, Reis ESC.** 2019. Slicing and dicing viruses: antiviral
520 RNA interference in mammals. *EMBO J* **38**.
- 521 6. **Li Y, Lu J, Han Y, Fan X, Ding SW.** 2013. RNA interference functions as an antiviral immunity
522 mechanism in mammals. *Science* **342**:231-234.
- 523 7. **Maillard PV, Ciaudo C, Marchais A, Li Y, Jay F, Ding SW, Voinnet O.** 2013. Antiviral RNA
524 interference in mammalian cells. *Science* **342**:235-238.
- 525 8. **Qiu Y, Xu Y, Zhang Y, Zhou H, Deng YQ, Li XF, Miao M, Zhang Q, Zhong B, Hu Y, Zhang FC, Wu
526 L, Qin CF, Zhou X.** 2017. Human Virus-Derived Small RNAs Can Confer Antiviral Immunity in
527 Mammals. *Immunity* **46**:992-1004 e1005.
- 528 9. **Xu YP, Qiu Y, Zhang B, Chen G, Chen Q, Wang M, Mo F, Xu J, Wu J, Zhang RR, Cheng ML,
529 Zhang NN, Lyu B, Zhu WL, Wu MH, Ye Q, Zhang D, Man JH, Li XF, Cui J, Xu Z, Hu B, Zhou X,
530 Qin CF.** 2019. Zika virus infection induces RNAi-mediated antiviral immunity in human neural
531 progenitors and brain organoids. *Cell Res* **29**:265-273.
- 532 10. **Li Y, Basavappa M, Lu J, Dong S, Cronkite DA, Prior JT, Reinecker HC, Hertzog P, Han Y, Li WX,
533 Cheloufi S, Karginov FV, Ding SW, Jeffrey KL.** 2016. Induction and suppression of antiviral
534 RNA interference by influenza A virus in mammalian cells. *Nat Microbiol* **2**:16250.
- 535 11. **Wu Q, Wang X, Ding SW.** 2010. Viral suppressors of RNA-based viral immunity: host targets.
536 *Cell Host Microbe* **8**:12-15.
- 537 12. **Chao JA, Lee JH, Chapados BR, Debler EW, Schneemann A, Williamson JR.** 2005. Dual modes
538 of RNA-silencing suppression by Flock House virus protein B2. *Nat Struct Mol Biol*
539 **12**:952-957.
- 540 13. **Li H, Li WX, Ding SW.** 2002. Induction and suppression of RNA silencing by an animal virus.
541 *Science* **296**:1319-1321.
- 542 14. **Lu R, Maduro M, Li F, Li HW, Broitman-Maduro G, Li WX, Ding SW.** 2005. Animal virus

- 543 replication and RNAi-mediated antiviral silencing in *Caenorhabditis elegans*. *Nature*
544 **436**:1040-1043.
- 545 15. **Qi N, Zhang L, Qiu Y, Wang Z, Si J, Liu Y, Xiang X, Xie J, Qin CF, Zhou X, Hu Y.** 2012. Targeting
546 of *dicer-2* and RNA by a viral RNA silencing suppressor in *Drosophila* cells. *J Virol*
547 **86**:5763-5773.
- 548 16. **Qi N, Cai D, Qiu Y, Xie J, Wang Z, Si J, Zhang J, Zhou X, Hu Y.** 2011. RNA binding by a novel
549 helical fold of *b2* protein from wuhan nodavirus mediates the suppression of RNA
550 interference and promotes *b2* dimerization. *J Virol* **85**:9543-9554.
- 551 17. **Nayak A, Kim DY, Trnka MJ, Kerr CH, Lidsky PV, Stanley DJ, Rivera BM, Li KH, Burlingame AL,**
552 **Jan E, Frydman J, Gross JD, Andino R.** 2018. A Viral Protein Restricts *Drosophila* RNAi
553 Immunity by Regulating Argonaute Activity and Stability. *Cell Host Microbe* **24**:542-557.e549.
- 554 18. **Haasnoot J, de Vries W, Geutjes EJ, Prins M, de Haan P, Berkhout B.** 2007. The Ebola virus
555 VP35 protein is a suppressor of RNA silencing. *PLoS Pathog* **3**:e86.
- 556 19. **Bennasser Y, Le SY, Benkirane M, Jeang KT.** 2005. Evidence that HIV-1 encodes an siRNA and
557 a suppressor of RNA silencing. *Immunity* **22**:607-619.
- 558 20. **Chen W, Zhang Z, Chen J, Zhang J, Zhang J, Wu Y, Huang Y, Cai X, Huang A.** 2008. HCV core
559 protein interacts with Dicer to antagonize RNA silencing. *Virus Res* **133**:250-258.
- 560 21. **Kakumani PK, Ponia SS, S RK, Sood V, Chinnappan M, Banerjea AC, Medigeshi GR, Malhotra**
561 **P, Mukherjee SK, Bhatnagar RK.** 2013. Role of RNA interference (RNAi) in dengue virus
562 replication and identification of NS4B as an RNAi suppressor. *J Virol* **87**:8870-8883.
- 563 22. **Samuel GH, Wiley MR, Badawi A, Adelman ZN, Myles KM.** 2016. Yellow fever virus capsid
564 protein is a potent suppressor of RNA silencing that binds double-stranded RNA. *Proc Natl*
565 *Acad Sci U S A* **113**:13863-13868.
- 566 23. **Karjee S, Minhas A, Sood V, Ponia SS, Banerjea AC, Chow VT, Mukherjee SK, Lal SK.** 2010.
567 The 7a accessory protein of severe acute respiratory syndrome coronavirus acts as an RNA
568 silencing suppressor. *J Virol* **84**:10395-10401.
- 569 24. **Cui L, Wang H, Ji Y, Yang J, Xu S, Huang X, Wang Z, Qin L, Tien P, Zhou X, Guo D, Chen Y.** 2015.
570 The Nucleocapsid Protein of Coronaviruses Acts as a Viral Suppressor of RNA Silencing in
571 Mammalian Cells. *J Virol* **89**:9029-9043.
- 572 25. **Anonymous.** 1994. The alphaviruses: gene expression, replication, and evolution. 1994.
573 *Microbiol Rev* **58**:806.
- 574 26. **McCarthy MK, Morrison TE.** 2016. Chronic chikungunya virus musculoskeletal disease: what
575 are the underlying mechanisms? *Future Microbiol* **11**:331-334.
- 576 27. **Liu X, Tharmarajah K, Taylor A.** 2017. Ross River virus disease clinical presentation,
577 pathogenesis and current therapeutic strategies. *Microbes Infect* **19**:496-504.
- 578 28. **Laine M, Luukkainen R, Toivanen A.** 2004. Sindbis viruses and other alphaviruses as cause of
579 human arthritic disease. *J Intern Med* **256**:457-471.
- 580 29. **Yuan Z.** 2018. Investigation of Viral Pathogen Profiles in Some Natural Hosts and Vectors in
581 China. *Virol Sin* **33**:1-4.
- 582 30. **Quetglas JI, Ruiz-Guillen M, Aranda A, Casales E, Bezunartea J, Smerdou C.** 2010. Alphavirus
583 vectors for cancer therapy. *Virus Res* **153**:179-196.
- 584 31. **Samuel GH, Adelman ZN, Myles KM.** 2018. Antiviral Immunity and Virus-Mediated
585 Antagonism in Disease Vector Mosquitoes. *Trends Microbiol* **26**:447-461.
- 586 32. **Xia H, Wang Y, Atoni E, Zhang B, Yuan Z.** 2018. Mosquito-Associated Viruses in China. *Virol*

- 587 Sin **33**:5-20.
- 588 33. **Fros JJ, Pijlman GP.** 2016. Alphavirus Infection: Host Cell Shut-Off and Inhibition of Antiviral
589 Responses. *Viruses* **8**.
- 590 34. **Atkins GJ, Sheahan BJ, Dimmock NJ.** 1985. Semliki Forest virus infection of mice: a model for
591 genetic and molecular analysis of viral pathogenicity. *J Gen Virol* **66 (Pt 3)**:395-408.
- 592 35. **Mazzon M, Castro C, Thaa B, Liu L, Mutso M, Liu X, Mahalingam S, Griffin JL, Marsh M,
593 McInerney GM.** 2018. Alphavirus-induced hyperactivation of PI3K/AKT directs pro-viral
594 metabolic changes. *PLoS Pathog* **14**:e1006835.
- 595 36. **Kim KH, Rumenapf T, Strauss EG, Strauss JH.** 2004. Regulation of Semliki Forest virus RNA
596 replication: a model for the control of alphavirus pathogenesis in invertebrate hosts. *Virology*
597 **323**:153-163.
- 598 37. **Rupp JC, Sokoloski KJ, Gebhart NN, Hardy RW.** 2015. Alphavirus RNA synthesis and
599 non-structural protein functions. *J Gen Virol* **96**:2483-2500.
- 600 38. **Wengler G.** 2009. The regulation of disassembly of alphavirus cores. *Arch Virol* **154**:381-390.
- 601 39. **Zheng Y, Kielian M.** 2015. An alphavirus temperature-sensitive capsid mutant reveals stages
602 of nucleocapsid assembly. *Virology* **484**:412-420.
- 603 40. **Choi HK, Lu G, Lee S, Wengler G, Rossmann MG.** 1997. Structure of Semliki Forest virus core
604 protein. *Proteins* **27**:345-359.
- 605 41. **Yang D, Buchholz F, Huang Z, Goga A, Chen CY, Brodsky FM, Bishop JM.** 2002. Short RNA
606 duplexes produced by hydrolysis with Escherichia coli RNase III mediate effective RNA
607 interference in mammalian cells. *Proc Natl Acad Sci U S A* **99**:9942-9947.
- 608 42. **Shan G, Li Y, Zhang J, Li W, Szulwach KE, Duan R, Faghihi MA, Khalil AM, Lu L, Paroo Z, Chan
609 AW, Shi Z, Liu Q, Wahlestedt C, He C, Jin P.** 2008. A small molecule enhances RNA
610 interference and promotes microRNA processing. *Nat Biotechnol* **26**:933-940.
- 611 43. **Mathur K, Anand A, Dubey SK, Sanan-Mishra N, Bhatnagar RK, Sunil S.** 2016. Analysis of
612 chikungunya virus proteins reveals that non-structural proteins nsP2 and nsP3 exhibit RNA
613 interference (RNAi) suppressor activity. *Sci Rep* **6**:38065.
- 614 44. **Lu R, Folimonov A, Shintaku M, Li WX, Falk BW, Dawson WO, Ding SW.** 2004. Three distinct
615 suppressors of RNA silencing encoded by a 20-kb viral RNA genome. *Proc Natl Acad Sci U S A*
616 **101**:15742-15747.
- 617 45. **Anandalakshmi R, Pruss GJ, Ge X, Marathe R, Mallory AC, Smith TH, Vance VB.** 1998. A viral
618 suppressor of gene silencing in plants. *Proc Natl Acad Sci U S A* **95**:13079-13084.
- 619 46. **Jose J, Snyder JE, Kuhn RJ.** 2009. A structural and functional perspective of alphavirus
620 replication and assembly. *Future Microbiol* **4**:837-856.
- 621 47. **Manfre AJ, Simon AE.** 2008. Importance of coat protein and RNA silencing in satellite
622 RNA/virus interactions. *Virology* **379**:161-167.
- 623 48. **Korber S, Shaik Syed Ali P, Chen JC.** 2009. Structure of the RNA-binding domain of Nodamura
624 virus protein B2, a suppressor of RNA interference. *Biochemistry* **48**:2307-2309.
- 625 49. **Miao M, Yu F, Wang D, Tong Y, Yang L, Xu J, Qiu Y, Zhou X.** 2019. Proteomics Profiling of Host
626 Cell Response via Protein Expression and Phosphorylation upon Dengue Virus Infection. *Virology*
627 Sin doi:10.1007/s12250-019-00131-2.
- 628 50. **Dai S, Zhang T, Zhang Y, Wang H, Deng F.** 2018. Zika Virus Baculovirus-Expressed Virus-Like
629 Particles Induce Neutralizing Antibodies in Mice. *Virology* **33**:213-226.
- 630

631 **Figure legends**

632 **Figure 1. SFV capsid protein is a potential VSR.** (A) S2 cells were co-transfected
633 with a plasmid encoding EGFP (0.1 µg) and dsEGFP (0.3 µg), together with either
634 empty plasmid or a plasmid encoding SFV protein or FHV B2 (FB2) (1 µg for each).
635 At 48 h.p.t., total RNAs were extracted and the level of EGFP mRNA was examined
636 via Northern blotting with a DIG-labeled RNA probe targeting 500-720 nt of EGFP
637 ORF region. Rp49 mRNA was used as loading control. (B) The expression of SFV
638 proteins was detected by Western blotting. (C) S2 cells were transfected with pMT
639 FHV RNA1 (FHV RNA1) (0.01 µg) or pMT FHV ΔB2 RNA1 (FR1 ΔB2) (0.3 µg)
640 and together with a plasmid encoding SFV capsid or FB2 as indicated above. At 48
641 h.p.t., FHV RNA transcription was induced by incubation with CuSO₄ (0.5 mM). At
642 24 hours after induction, total RNAs were harvested for Northern blot analysis. The
643 band between RNA1 and RNA3 was the B2 mRNA transcribed from expression
644 plasmid. The dsRNAs targeting AGO2 (dsAGO2) and Dicer2 (dsDicer2) were used as
645 positive controls. (D) 293T cells were co-transfected with a plasmid encoding EGFP
646 (0.1 µg), EGFP-specific shRNA (shEGFP) (0.3 µg) together with either empty
647 plasmid or a plasmid encoding SFV capsid protein, nsP2, nsP3 or NB2 (1 µg for each).
648 At 48 h.p.t., total RNAs were extracted and the level of EGFP mRNA was examined
649 via Northern blotting. (E) The expression of SFV nsP2, nsP3 and capsid proteins in
650 293T cells was detected by Western blotting. (F) S2 cells were co-transfected with a
651 plasmid encoding EGFP (0.1 µg), EGFP-dsRNA (dsEGFP) (0.3 µg) together with
652 either empty plasmid or a plasmid encoding SINV capsid protein, SFV capsid protein,
653 or FB2 (1 µg for each). At 48 h.p.t., total RNAs were extracted and the level of EGFP
654 mRNA was examined via Northern blotting. Rp49 mRNA was used as the loading
655 control. (G) 293T cells were co-transfected with a plasmid encoding EGFP (0.1 µg),
656 EGFP-specific shRNA (shEGFP) (0.3 µg) together with either empty plasmid or a
657 plasmid encoding SINV capsid protein, SFV capsid protein, or NB2 (1 µg for each).
658 At 48 h.p.t., total RNAs were extracted and the level of EGFP mRNA was examined
659 via Northern blotting. GAPDH mRNA was used as the loading control.

660

661 **Figure 2. SFV capsid suppresses Dicer-mediated siRNA production by**
662 **sequestering dsRNA. (A)** 293T cells were co-transfected with a plasmid encoding
663 EGFP (0.1 μ g), EGFP-specific shRNA (shEGFP) (0.3 μ g), together with either empty
664 plasmid or a plasmid encoding SFV capsid protein or NB2 (1 μ g for each). At 48
665 h.p.t., total RNAs were extracted for small Northern blotting with a DIG-labeled RNA
666 oligo probe targeting EGFP siRNA. U6 was used as the loading control. **(B)**
667 SDS-PAGE of purified recombinant SFV capsid. BSA was used as a quantity control.
668 **(C)** Increasing amount (0-4 μ M) of MBP-fusion capsid (MBP-capsid) was incubated
669 with 0.5 μ M 200 nt DIG-labeled dsRNA at 25°C for 30 min. Complexes were
670 separated on 1.5% native-TBE agarose gel, transferred to membranes, and then
671 incubated with anti-DIG antibody conjugated with alkaline phosphatase. MBP-FB2
672 and MBP were used as the controls. **(D)** Increasing amount (0-4 μ M) of MBP-capsid
673 was incubated with 1 μ M 200-nt DIG-labeled dsRNA at 25°C for 30 min. Then the
674 protein-dsRNA complexes were incubated with 1 U RNase III at 37°C for 30 min.
675 The reaction products were subjected to 7 M urea-15% PAGE analysis.

676

677 **Figure 3. SFV capsid suppresses siRNA-induced RNAi. (A)** 293T cells were
678 co-transfected with a plasmid encoding EGFP (0.1 μ g), EGFP-specific siRNA
679 (siEGFP) (50 nM), together with either empty plasmid or a plasmid encoding SFV
680 capsid protein or NB2 (1 μ g for each). At 48 h.p.t., total RNAs were extracted for
681 Northern blotting. GAPDH mRNA was used as the loading control. **(B)** Increasing
682 amount (0-8 μ M) of MBP-fusion capsid was incubated with 1 μ M DIG-labeled
683 synthetic 22-nt siRNA at 25°C for 30 min. Complexes were separated on 1.5%
684 native-TBE agarose gel, transferred to membranes, and then incubated with anti-DIG
685 antibody conjugated with alkaline phosphatase.

686

687 **Figure 4. K124/K128 and K139/K142 of SFV capsid are critical for theVSR**
688 **activity. (A-B)** S2 cells were co-transfected with a plasmid encoding EGFP (0.1 μ g)

689 and dsEGFP (0.3 μ g), together with either empty plasmid or a plasmid encoding SFV
690 capsid deletion mutant as indicated or FB2 (1 μ g for each). At 48 h.p.t., total RNAs
691 were extracted for Northern blotting. Rp49 mRNA was used as the loading control.
692 The expression of capsid mutations in S2 cells was detected by Western blotting (B).
693 **(C-D)** The amino acid sequence alignment of alphaviral capsids are as follows: SFV4
694 (KP699763.1), SFV6 (KT009012.1), SFV-L10 (KP271965.1), SFV-A7 (Z48163.2),
695 CHIKV (AOT86261.1), RRV (P08491.3), SINV (AKZ17419.1). S2 cells were
696 co-transfected with a plasmid encoding EGFP (0.1 μ g) and dsEGFP (0.3 μ g), together
697 with either empty plasmid or the plasmid encoding the indicated single-point
698 mutations of SFV capsid (1 μ g for each). At 48 h.p.t., total RNAs were extracted for
699 Northern blotting. The expression of capsid mutations in S2 cells was detected by
700 Western blotting (D). **(E-G)** Schematic illustration of double-point mutations of SFV
701 capsid. S2 cells were co-transfected with a plasmid encoding EGFP (0.1 μ g) and
702 dsEGFP (0.3 μ g), together with either empty plasmid or the plasmid encoding the
703 indicated double-point mutations of SFV capsid (1 μ g for each). At 48 h.p.t., total
704 RNAs were extracted for Northern blotting (E) and qRT-PCR (G). The expression of
705 capsid mutations in S2 cells was detected by Western blotting (F). **(H-I)** 293T cells
706 were co-transfected with a plasmid encoding EGFP (0.1 μ g), EGFP-specific shRNA
707 (shEGFP) (0.3 μ g) together with either empty plasmid or a plasmid encoding SFV
708 capsid protein or mutations, NB2 (1 μ g for each). At 48 h.p.t., total RNAs were
709 extracted and the level of EGFP mRNA was examined via Northern blotting. GAPDH
710 mRNA was used as the loading control. The expression of capsid mutations in 293T
711 cells was detected by Western blotting (I). **(J-K)** 293T cells were co-transfected with
712 a plasmid encoding EGFP (0.1 μ g), EGFP-specific siRNA (siEGFP) (0.3 μ g) together
713 with either empty plasmid or a plasmid encoding capsid_{WT}, capsid_{K124A/K128A},
714 capsid_{K139A/K142A}, or NB2 (1 μ g for each). At 48 h.p.t., total RNAs were extracted and
715 the level of EGFP mRNA was examined via Northern blotting. The expression of
716 capsid mutations in 293T cells was detected by Western blotting (K).
717

718 **Figure 5. K124/K128 and K139/K142 of SFV capsid are critical for the dsRNA-**
719 **and siRNA-binding.** (A-C) MBP-capsid_{WT}, MBP-capsid_{K124A/K128A}, or
720 MBP-capsid_{K139A/K142A} was incubated with 0.5 μ M 200-nt DIG-labeled dsRNA (A), 1
721 μ M 22-nt siRNA (B) or 0.5 μ M ssRNA (C) at 25°C for 30 min. The complexes were
722 separated on 1.5% native-TBE agarose gel, transferred to membranes, and then
723 incubated with anti-DIG antibody conjugated with alkaline phosphatase. MBP-FB2
724 and MBP alone were used as positive and negative control, respectively.

725

726 **Figure 6. Construction and recovery of VSR-deficient SFV.** (A) SFV genome and
727 the mutation sites of K124A/K128A and K139A/K142A. (B) The plaque morphology
728 of SFV_{WT} and SFV_{K124A/K128A}. (C) The virions of SFV_{WT} and SFV_{K124A/K128A} was
729 examined via TEM with magnification times 40000. (D) 293T cells were infected
730 with SFV_{WT} and SFV_{K124A/K128A} at an MOI of 5. At 15, 30 and 45 minutes post
731 infection, the viruses remaining in the supernatant and the viral RNAs entered into
732 cells were examined by plaque assays and qRT-PCR, respectively. The RNA levels of
733 SFV_{K124A/K128A} in 293T cells at 15 minutes post infection was defined as 1. All data
734 represent means and SD of three independent experiments. n.s., not significant. (E)
735 293T cells were infected with SFV_{WT} or SFV_{K124A/K128A} (MOI=0.1), respectively.
736 Viral titers were measured at the indicated times using standard plaque assay in Vero
737 cells. All data represent means and SD of three independent experiments. * p <0.05,
738 ** p <0.01 as measured by two-way ANOVA (GraphPad Prism).

739

740 **Figure 7. The deficiency of RNAi rescued the defective replication of**
741 **VSR-deficient SFV.** (A) 293T or 293T-NoDice cells were transfected with either
742 empty plasmid or a plasmid encoding NoV B2, mB2 (B2_{R59Q}), SFV capsid or
743 capsid_{K124A/K128A} as indicated. At 24 h.p.t., cells were infected with SFV_{WT} or
744 SFV_{K124A/K128A} at an MOI of 1. At 6, 12, and 24 h.p.i., the levels of SFV genomic
745 RNAs in cells were determined by qRT-PCR, and the level of SFV_{K124A/K128A} RNA in
746 293T cells at 6 h.p.i. was defined as 1. All data represent means and SD of three

747 independent experiments. * $p < 0.05$, ** $p < 0.01$, *** $p < 0.001$ as measured by two-way
748 ANOVA (GraphPad Prism). **(B)** 293T or NoDice 293T cells were transfected with
749 either empty plasmid or a plasmid encoding human Dicer (hDicer) as indicated. At 24
750 h.p.t., cells were treated with Enoxacin (100 μM) for 1h and then infected with SFV_{WT}
751 at an MOI of 1. At 6, 12, and 24 h.p.i., the levels of SFV genomic RNAs in cells were
752 determined by qRT-PCR, and the level of SFV_{K124A/K128A} RNA in 293T cells treated
753 with DMSO at 6 h.p.i. was defined as 1. All data represent means and SD of three
754 independent experiments. **(C-D)** The expression of capsid, capsid_{K124A/K128A}, NoV B2,
755 mB2 or hDicer proteins in 293T or 293T-NoDice cells was detected by Western
756 blotting. **(E)** 293T cells were transfected with SFV capsid or capsid_{K124A/K128A} as
757 indicated, and then infected with SFV_{WT} or SFV_{K124A/K128A} at an MOI of 1. At 24
758 h.p.i., the total RNAs were extracted, the level of SFV genomic and subgenomic RNAs
759 were examined via Northern blotting with DIG-labeled RNA probe targeting
760 723-1314 nt of SFV E2 coding region. GAPDH mRNA was used the loading control.
761 **(F)** 293T-NoDice cells were transfected with either empty plasmid or a plasmid
762 encoding NoV B2, SFV capsid as indicated. At 24 h.p.t., cells were infected with
763 SFV_{K124A/K128A} at an MOI of 1. At 6, 12, and 24 h.p.i., the levels of SFV genomic
764 RNAs in cells were determined by qRT-PCR, and the level of SFV_{K124A/K128A} RNA in
765 293T cells transfected with either empty plasmid at 6 h.p.i. was defined as 1. **(G)** The
766 expression of SFV capsid, and NoV B2 in 293T-NoDice cells was detected by
767 Western blotting. **(H)** 293T or 293T-NoDice cells were transfected with either empty
768 plasmid or a plasmid encoding NoV B2, mB2 (B2_{R59Q}), SFV capsid or
769 capsid_{K124A/K128A} as indicated. At 24 h.p.t., cells were treated with Ruxolitinib (10 μM)
770 for 1h and then infected with SFV_{WT} or SFV_{K124A/K128A} at an MOI of 1. At 6, 12, and
771 24 h.p.i., the levels of SFV genomic RNAs in cells were determined by qRT-PCR,
772 and the level of SFV_{K124A/K128A} RNA in 293T cells at 6 h.p.i. was defined as 1. **(I)** The
773 expression of capsid, capsid_{K124A/K128A}, NoV B2, or mB2 in Ruxolitinib treated 293T
774 cells was detected by Western blotting. **(J)** Aag2 cells were infected with SFV_{WT} or
775 SFV_{K124A/K128A} at an MOI of 1. At 6, 12, and 24 h.p.i., the levels of SFV genomic

776 RNAs in cells were determined by qRT-PCR, and the level of SFV_{K124A/K128A} RNA in
777 MLF cells at 6 h.p.i. was defined as 1. (K) Aag2 cells were infected with SFV_{WT} or
778 SFV_{K124A/K128A} at an MOI of 10. At 24 h.p.i., total RNAs were extracted, and the
779 levels of vsiRNAs were examined via Northern blotting with a DIG-labeled RNA
780 probe targeting 1-50 nt of antigenomic SFV RNA. U6 was used a loading control.

781

782 **Figure 8. Model for the suppression of RNAi in mammalian and mosquito cells**
783 **by SFV capsid protein.** When SFV entry the host cells, the single-stranded genomic
784 (+)RNAs are used as the templates to produce the negative genomic (-)RNAs. Then
785 the (-)RNAs can be used as the templates to produce more progeny (+)RNAs and
786 subgenomic RNAs. The vRI-dsRNAs formed by the 5'-terminal nascent (+)RNAs
787 or/subgenomic RNAs and the (-)RNA template could be recognized and cleaved by
788 Dicer, thus triggering antiviral RNAi. SFV capsid protein can suppress antiviral RNAi
789 by sequestering dsRNA and siRNA as indicated.

Table 1. The primers and oligonucleotides used in this study.

Primers for construction of SFV proteins

Name	Sequence	Restriction enzyme
pAc-v5/His-NS1-anti	GAATTCTATGGCCGCCAAAGTGCATGTTGATAT	EcoR I
pAc-v5/His-NS1-anti	CTCGAGCGTGCACCTGCGTGATACTCTAGTTC	Xho I
pAc-v5/His-NS2-sense	GCGGCCGCATGGGGTTCGTGGAAACACCTCGCA	Not I
pAc-v5/His-NS2-anti	TCTAGACTACACCCGGCCGTGTGCATGGCTTCTC	Xba I
pAc-v5/His-NS3-sense	GAATTCTATGGCACCATCCTACAGAGTTAAGAGAGC	EcoR I
pAc-v5/His-NS3-anti	TCTAGACTTGCACCCGCGCGCCTAGTCGCAGGAC	Xba I
pAc-v5/His-NS4-sense	GAATTCTATGTATATTTCTCCTCGGACACACTGGCA	EcoR I
pAc-v5/His-NS4-anti	CTCGAGCGACGCACCAATCTAGGACCGCCGTAGAG	Xho I
pAc-v5/His-capsid-sense	GCGGCCGCATGAATTACATCCCTACGCAAACGTTTT	Not I
pAc-v5/His-capsid-anti	CTCGAGCGCCACTCTTCGGACCCCTCGGGGGTCA	Xho I
pAc-v5/His-E3-sense	GAATTCTATGTCCGCCCCGCTGATTACTGCCATGT	EcoR I
pAc-v5/His-E3-anti	TCTAGAGCGCCGGTGTCTTGTTCGGTTCGGCAGC	Xba I
pAc-v5/His-E2-sense	GCGGCCGCATGAGCGTGTGCAACACTTCAACGTG	Not I
pAc-v5/His-E2-anti	CTCGAGCGTGCCTGCGCCCGGGGCGCAGCAGAG	Xho I
pAc-v5/His-6k-sense	GCGGCCGCCATGGCTAGTGTGGCAGAGACTATGGC	Not I
pAc-v5/His-6k-anti	CTCGAGCGAGCTCTGGCGTTGCCCGAGGCTCAGT	Xho I
pAc-v5/His-E1-sense	GCGGCCGCATGTACGAACATTCGACAGTAATGCCGA	Not I
pAc-v5/His-E1-anti	CTCGAGCGTCTGCGGAGCCCAATGCAAGTGACCACA	Xho I
pRK-capsid-sense	GTCGACGATGAATTACATCCCTACGCAAACGTTTTAC	Sal I
pRK-capsid-anti	GCGGCCGCTTACCCTCTTCGGACCCCTCGGGGGTCA	Not I
pMal-c2x-capsid-sense	GAATTCATGAATTACATCCCTACGCAAACGTTTTAC	EcoR I
pMal-c2x-capsid-anti	GTCGACCCACTCTTCGGACCCCTCGGGGGTCACTC	Sal I

Primers for construction of capsid mutants and SFV mutant

Name	Sequence	Restriction enzyme
K124A/K128A-sense	TCTTCGAAGTCGCACACGAAGGAGCGGTCCTGG	-
K124A/K128A-anti	CCAGTGACCGCTCCTTCGTGTGCGACTTCGAAGA	-
K139A/K142A-sense	GCCTGGTGGGCGACGCAGTCATGGCACCTGCCCA	-
K139A/K142A-anti	TGGGCAGGTGCCATGACTGCGTCGCCACCAGGC	-
pMD18-T- K124A/K128A-sense	TCTAGAGACGGACATTGCATCATTC	Xba I
pMD18-T- K124A/K128A-anti	CCTGCAGGAATTCACCCGGTGGGCA	Sbf I

Primers for qRT-PCR

Name	Sequence
EGFP-sense	GACAAGCAGAAGAACGGCATC
EGFP-anti	CGGACTGGGTGCTCAGGTA
SFV-sense	CCGGAGGACGCACAGAAGTTG
SFV-anti	TGCGACGGCCACAATCGGAAG
Human actin-sense	AGAGCTACGAGCTGCTGAC
Human actin-anti	AGCACTGTGTTGGCGTACAG

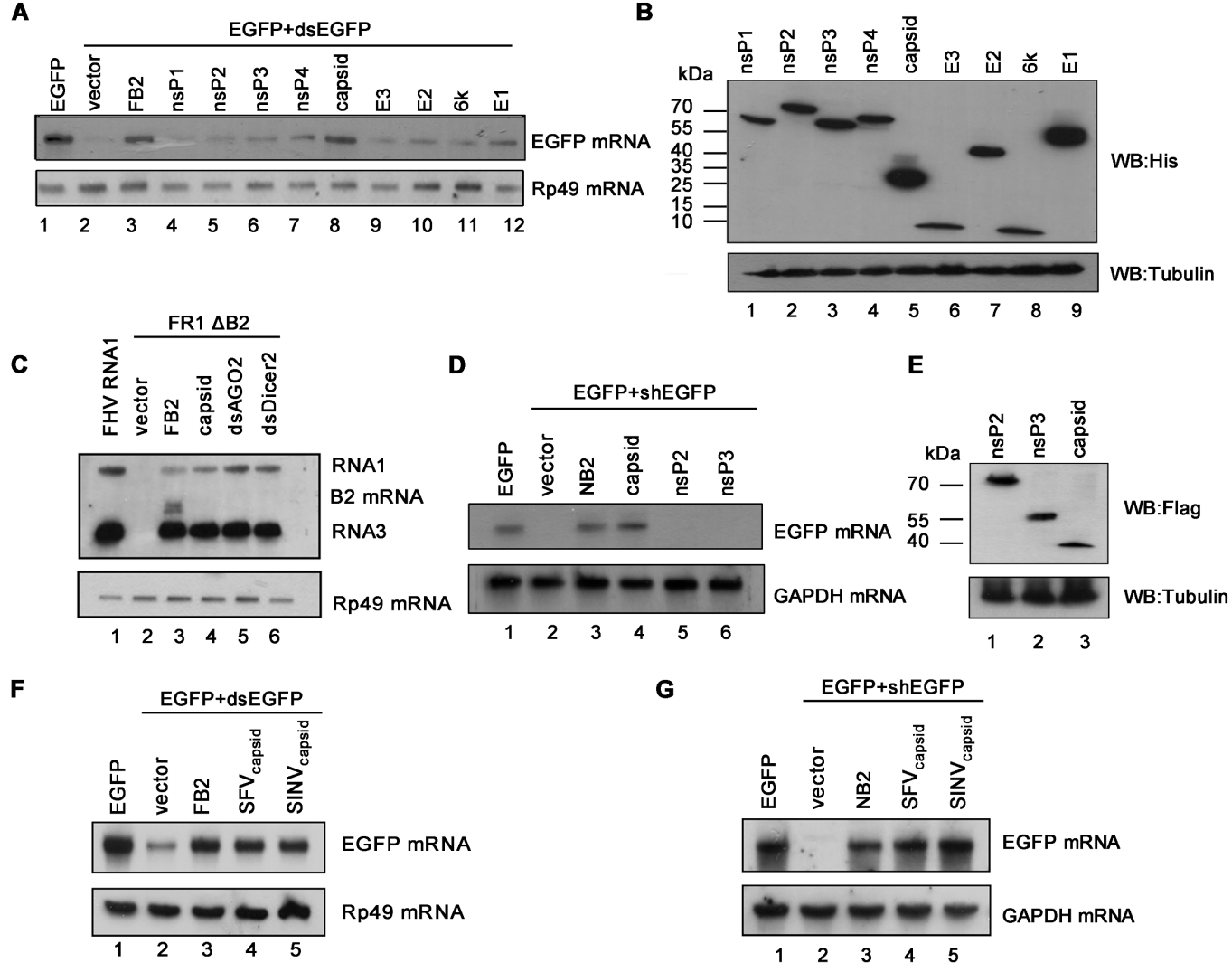
Aedes aegypti Rp49-sense	GCTATGACAAGCTTGCCCCCA
Aedes aegypti Rp49-anti	TCATCAGCACCTCCAGCT

Primers for amplification of templates for *in vitro* transcription dsRNAs and ssRNAs

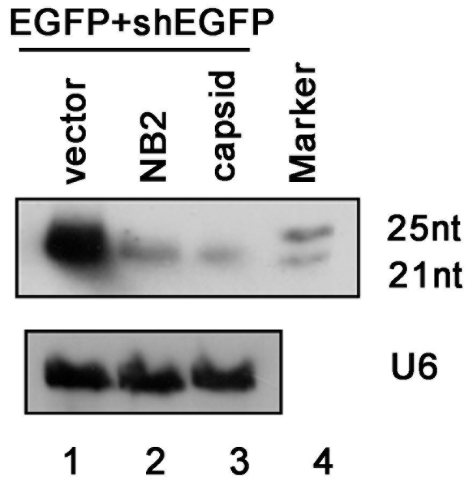
Name	Sequence
EGFP-ds400-sense	TAATACGACTCACTATAGATGGTGAGCTAGGGCGAGGA
EGFP-ds400-anti	TAATACGACTCACTATAGGCTTGTGCCCCAGGATGTTGC
EGFP-ds200-sense	TAATACGACTCACTATAGATGGTGAGCTAGGGCGAGGA
EGFP-ds200-anti	TAATACGACTCACTATAGGCGGCTGAAGCACTGCACGC
dsAgo2-sense	TAATACGACTCACTATAGATGGGAAAAAAGATAAGAACAAGC
dsAgo2-anti	TAATACGACTCACTATAGCACCTTGTGACCTGTTTAGTCCAC
EGFP-ss200-sense	TAATACGACTCACTATAGATGGTGAGCTAGGGCGAGGA
EGFP-ss200-anti	CTATAGTGAGTCGTATTAGCGGCTGAAGCACTGCACGC

Primers for amplification of templates for *in vitro* transcription RNA probes

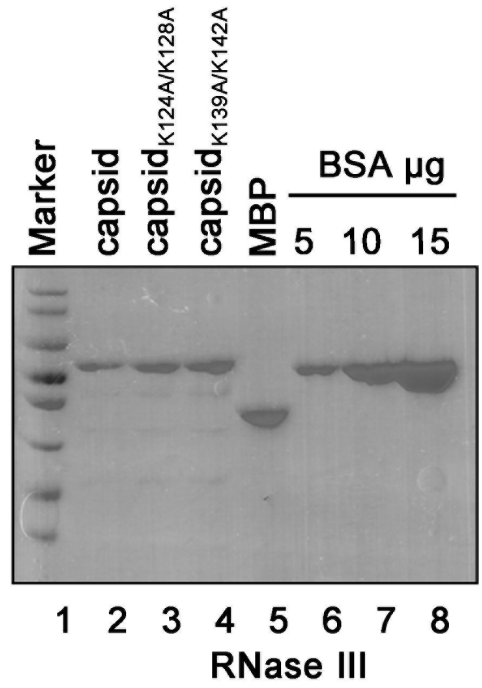
Name	Sequence
EGFP-probe-sense	GATCCGCCACAACATCGAGGACGGC
EGFP-probe-anti	TAATACGACTCACTATAGTACTTGTACAGCTCGTCCATGCC
S2-Rp49-sense	CCGTGAATACTGTGGTGAAATTGCC
S2-Rp49-anti	TAATACGACTCACTATAGGTTTTTTTTTTCACTTTTAACGTTTCA
GAPDH-probe-sense	GGCGTGATGGCCGCGGGCTCTCC
GAPDH-probe-anti	TAATACGACTCACTATAGGCAAAGGTGGAGGAGTGGGTGTCGC
SFV-probe-sense	GCTGCCAAATCAAACGAACCCGTGCAG
SFV-probe-anti	TAATACGACTCACTATAGGTCTGCGGAGCCCAATGCAAGTGACC
FHV-probe-sense	ATGCCAAGCAAACCTCGCGCTAATCCAGGAACCTCCCG
FHV-probe-anti	TAATACGACTCACTATAGGCCTCTAGGTATGCCACCACGCTGGGTTTCTC
siEGFP-sense	GCUGACCCUGAAGUUCAUCUU
siEGFP-anti	GAUGAACUUCAGGGUCAGCUU
SFV-vsiRNA-probe-sense	TAATACGACTCACTATAGATGGCGGATGTGTGACATACACGACGCCAAAAGATTTTGTCCA GCTCCT
SFV-vsiRNA-probe-anti	AGGAGCTGGAACAAAATCTTTTGGCGTCGTGTATGTACACATCCGCATCTATAGTGAGTC GTATTA



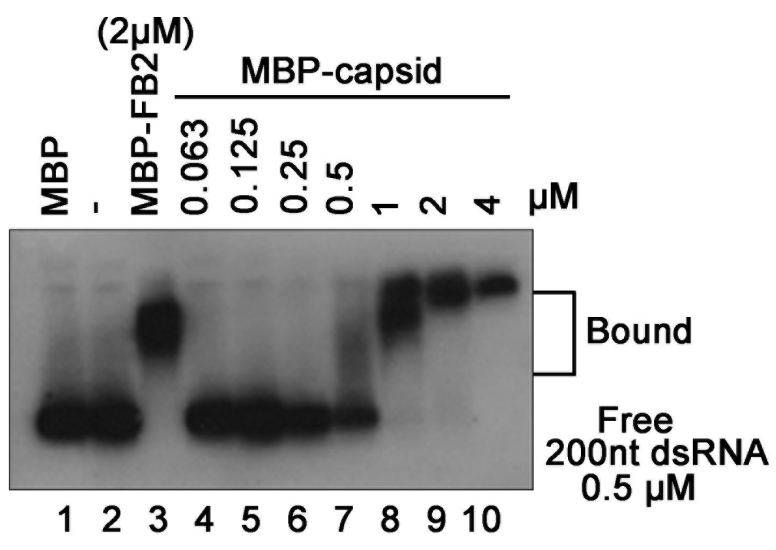
A



B



C



D

